Hormonal activity of AIMP1/p43 for glucose homeostasis

Sang Gyu Park*, Young Sun Kang*, Jin Young Kim*, Chang Seok Lee†, Young Gyu Ko†, Woo Je Lee‡, Ki-Up Lee‡, Young Il Yeom§, and Sunghoon Kim*§¶

*National Creative Research Initiatives Center for ARS Network, College of Pharmacy, Seoul National University, Seoul 151-742, Korea; †Division of Life Sciences and Graduate School of Biotechnology, Korea University, 1, 5-ga, Anam-dong, Sungbuk-gu, Seoul 136-701, Korea; ‡Department of Internal Medicine, University of Ulsan College of Medicine, Seoul 138-736, Korea; and §Genome Research Center, Korea Research Institute of Bioscience and Biotechnology, Daejon 305-333, Korea

Edited by Lewis T. Williams, Five Prime Therapeutics, San Francisco, CA, and approved August 2, 2006 (received for review March 14, 2006)

AIMP1/p43 is known as a cytokine working in the control of angiogenesis, inflammation, and wound healing. Here we report its enrichment in pancreatic α cells and glucagon-like hormonal activity. AIMP1 is secreted from the pancreas upon glucose starvation. Exogenous infusion of AIMP1 increased plasma levels of glucose, glucagon, and fatty acid, and AIMP1-deficient mice showed reduced plasma glucose levels compared with the wild-type mice under fasting conditions. Thus, AIMP1 plays a glucagon-like role in glucose homeostasis.

aminoacyl-tRNA synthetase | glucagon | pancreas

AIMP1 (ARS-interacting multifunctional protein 1) was first identified as an auxiliary factor bound to the multi-ARS (aminoacyl-tRNA synthetase) complex (1–4). AIMP1 interacts with arginyl-tRNA synthetase to enhance its enzymatic activity (5). AIMP1 is also secreted (6), and its secretion is induced by various stimulations, such as TNFα and heat shock (7, 8). The secreted AIMP1 has a variety of functions. First, AIMP1 controls angiogenesis with a dual mechanism (9). Low concentrations of AIMP1 induce the matrix metalloproteinase type 9-mediated angiogenesis, whereas high concentrations enhance JNK-mediated anti-angiogenesis. Second, AIMP1 induces inflammation through the activation of monocytes/macrophages (6, 7). AIMP1 also induces homotypic immune cell adhesion via induction of intercellular adhesion molecule 1 (10). Third, AIMP1 enhances wound closure through fibroblast proliferation and collagen synthesis (7). Here we report the additional activity of AIMP1 in the regulation of glucose metabolism. The free form of AIMP1 is enriched in pancreatic α cells and is secreted by hypoglycemic stimulation to increase the blood concentrations of glucagon, glucose, and fatty acid.

Results

Pancreatic Localization of AIMP1. To explore the additional activity of AIMP1, we examined the tissue-dependent variation of AIMP1 level. Whereas methionyl-tRNA synthetase and glutaminyl-tRNA synthetase showed relatively similar levels, the AIMP1 level showed significant tissue-dependent variation with high enrichment in salivary glands and the pancreas (Fig. 1*A*). Because AIMP1 exists as a component of the macromolecular tRNA synthetase complex, we checked whether some portion of AIMP1 would exist as a free form that is not bound to the complex in the tissues containing high concentrations of AIMP1 using sizing chromatography. Although AIMP1 was mainly eluted in the complex-bound form in the lung with other components such as glutamyl-prolyl-tRNA synthetase and prolyl-tRNA synthetase, it was eluted in both complex-bound and free forms in the pancreas, where AIMP1 levels were high (Fig. 1*B*).

Because the pancreas is an exo- and endocrine gland composed of different types of secretory cells, we further sought to determine the types of cells responsible for the enrichment of AIMP1 in the pancreas. Immunofluorescence staining of AIMP1 revealed that it is specifically localized to the peripheral area of the pancreatic islets (Fig. 1*C*) (11, 12). We further dissected the localization of AIMP1 between α and β cells within islets and found that AIMP1 was highly concentrated in α cells along with glucagon but not in β cells with insulin (Fig. 1*D*). Through electron microscopic observation of AIMP1 we further found that AIMP1 is enriched in the secretory vesicles of the α cells of pancreatic islets (Fig. 1*E*). The secretory vesicles were confirmed by ImmunoGold staining of glucagon (data not shown).

Pancreatic Secretion of AIMP1 Is Induced by Low Glucose Levels. To see whether AIMP1 is actually secreted from α cells, we investigated the secretion of AIMP1 from the pancreas. Because AIMP1 is colocalized with glucagon, we expected that AIMP1 secretion could be controlled by the variation of blood glucose concentration. We introduced the glucose solution with different concentrations into mice by means of cardiac perfusion, isolated the pancreas, and incubated the pancreas in the medium to check whether AIMP1 is secreted by the change of glucose concentration. AIMP1 was secreted to the medium at glucose concentrations $<$100 mg/dl, but not above (Fig. 2*A*), indicating that AIMP1 is secreted upon low glucose concentrations. To confirm these results, we cultured a pancreatic α cell line, aTC1 clone 9, at high (450 mg/dl) and low (75 mg/dl) glucose concentrations, harvested the medium at different time points, and checked the AIMP1 secretion by Western blotting. AIMP1 was specifically secreted to medium at low glucose concentrations (75 mg/dl) with no change in its expression (Fig. 2*B*). We then tested whether the secreted AIMP1 would induce the glucagon secretion. Glucagon secretion was enhanced by AIMP1 treatment $\approx$3-fold from the pancreatic α cells in 15 min and subsequently declined to the background level (Fig. 2*C*). Combined, these findings indicate that AIMP1 is secreted at low plasma glucose levels and induces glucagon secretion.

Effects of AIMP1 on Plasma Levels of Glucagon and Glucose-Related Metabolites. Because AIMP1 was secreted at low glucose concentrations and induces the secretion of glucagon, it may work directly or indirectly via the secretion of glucagon to restore normal glucose levels in blood. To delineate this possibility, we infused recombinant AIMP1 into tail veins and monitored the blood level changes of various metabolites. The plasma glucagon

Author contributions: S.G.P., K.-U.L., Y.I.Y., and S.K. designed research; S.G.P., Y.S.K., J.Y.K., C.S.L., and Y.G.K. performed research; Y.G.K. contributed new reagents/analytic tools; S.G.P., W.J.L., and K.-U.L. analyzed data; and S.G.P. and S.K. wrote the paper.

The authors declare no conflict of interest.

This paper was submitted directly (Track II) to the PNAS office.

Abbreviation: IPGTT, i.p. glucose tolerance test.

¶To whom correspondence should be addressed. E-mail: sungkim@snu.ac.kr.

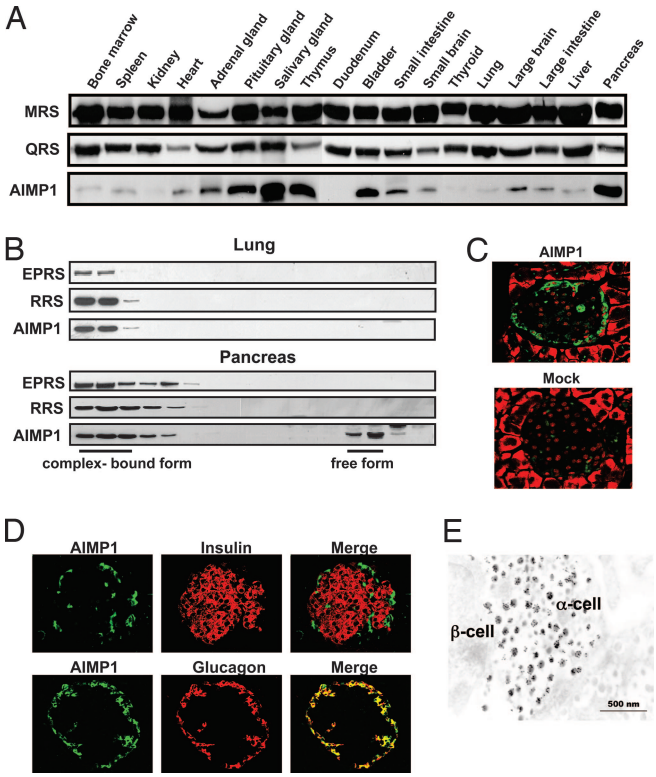

Fig. 1. Enriched localization of AIMP1 in pancreatic α cells. (*A*) Tissue-dependent variations of protein levels were determined for AIMP1 and two tRNA synthetases, methionyl-tRNA synthetase and glutaminyl-tRNA synthetase, which are components of the multi-tRNA synthetase complex. Proteins extracted from each tissue were subjected to Western blot analysis with their respective antibodies. (*B*) AIMP1 was separated into the portions that were bound and unbound to the multi-tRNA synthetase complex by size exclusion chromatography. The proteins extracted from the lung and pancreas that contained low and high levels of AIMP1, respectively, were compared. The two other components for the complex, glutamyl-prolyl-tRNA synthetase and arginyl-tRNA synthetase, were used as indicators for the complex-bound portion. The eluted proteins were resolved by SDS/PAGE, and three proteins were detected with their respective antibodies. (*C*) Localization of AIMP1 in the pancreatic islet was determined by immunofluorescence staining. AIMP1 and nuclei were stained green with FITC-conjugated antibody and red with propidium iodide, respectively. (Magnification: ×20.) (*D*) Colocalization of AIMP1 (green) in the pancreatic α cells with glucagon (red) under a confocal microscope. In *Upper*, pancreatic β cells were stained with insulin antibody and rhodamine-conjugated secondary antibody. (Magnification: ×20.) (*E*) A mouse pancreas was dissected and fixed as described in *Materials and Methods*. Grids were reacted with anti-AIMP1 antibody and detected with colloidal gold-conjugated protein A. The labeled sections were observed under an electron microscope (JEOL) at 80 kV.

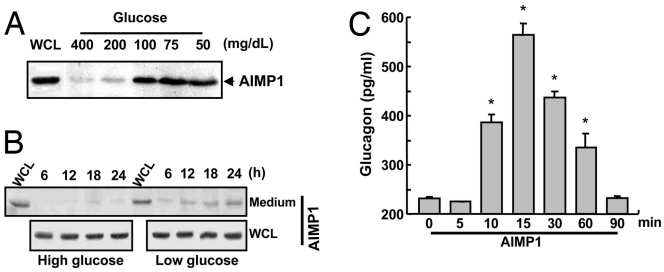

Fig. 2. Low glucose levels induce pancreatic secretion of AIMP1. (*A*) Secretion of AIMP1 by pancreatic stimulation through the cardiac perfusion of the conditioned medium containing the indicated concentrations of glucose. After perfusion of the glucose solution for 5 min at a flow rate of 10 ml/min, pancreases were isolated and incubated as described in *Materials and Methods*. The secreted proteins were precipitated from the harvested medium by the addition of 10% TCA, separated by 10% SDS/PAGE, and blotted with anti-AIMP1 antibody. WCL, whole-cell lysates. (*B*) We also confirmed that the secretion of AIMP1 is induced under hypoglycemic conditions (75 mg/dl) from aTC1 clone 9 but not under hyperglycemic conditions (450 mg/dl). (*C*) Glucagon secretion was stimulated by AIMP1 (100 nM) from aTC1 clone 9. The secreted glucagon was quantified by using an RIA kit (LINCO Research). The values are means ± SD. *, $P < 0.02$.

level was increased ≈3-fold after the AIMP1 infusion (Fig. 3*A*), whereas the insulin level was not affected (Fig. 3*B*). We also determined the change of the plasma glucose and lactate concentrations by AIMP1. AIMP1 raised the plasma glucose level ≈2-fold (Fig. 3*C*) but did not induce any change in the lactate concentration (Fig. 3*D*). Blood glucose showed a peak at 60 min and then gradually declined. Free fatty acid and glycerol showed a peak at 30 min after AIMP1 infusion and then returned to basal levels (Fig. 3 *E* and *F*). The AIMP1-induced increase of glucose before glucagon enhancement suggests that it could directly control the glucose level in addition to its stimulation of glucagon secretion.

AIMP1 Induces Glycogenolysis and Lipolysis. The metabolic action of AIMP1 may be achieved in two different ways. First, it could block the uptake of glucose, glycerol, and free fatty acid in peripheral tissues. This possibility was checked in adipocytes (3T3-L1), myocytes (C2C12), and hepatoma (HepG2). AIMP1 did not affect the uptake of [^{14}C]D-glucose and [^{3}H]palmitic acid in adipocytes and muscle cells (Fig. 6, which is published as supporting information on the PNAS web site). However, AIMP1 inhibited the uptake of D-glucose in HepG2 (Fig. 4*A*), but not the uptake of fatty acid (Fig. 4*B*). Because [^{14}C]D-glucose can be metabolized to different metabolites within the cells, we also monitored the glucose uptake using [^{14}C]D-deoxyglucose and observed a similar result (data not shown). AIMP1 can also induce the secretion of glucose, free fatty acid, and glycerol from peripheral tissues such as liver and adipose tissue. For the glucose secretion assay, we activated glycogen storage in HepG2 by insulin treatment in the presence of [U-^{14}C]D-glucose. We then treated the cells with AIMP1 to determine whether it enhances disgorgement of glucose through glycogenolysis. AIMP1 increased [U-^{14}C]D-glucose levels in the medium ≈3-fold in a dose-dependent manner (Fig. 4*C*), whereas the intracellular concentration of [U-^{14}C]D-glycogen decreased ≈20% (Fig. 4*D*). These data suggest that AIMP1 could induce glycogenolysis to supply glucose to blood while inhibiting glucose uptake in hepatocytes.

We then checked whether AIMP1 stimulates lipolysis in differentiated adipocytes by measuring the secretion of free fatty acid and glycerol because most of them are degradation products of triglyceride from adipose tissue. We induced storage of [^{3}H]palmitic acid into triglyceride by treating the differentiated adipocytes with insulin. We then treated the cells with different concentrations of AIMP1 for 8 h and measured [^{3}H]palmitic acid levels in the culture medium and cells. The concentration of [^{3}H]palmitic acid increased in the medium ≈4-fold by AIMP1 treatment (Fig. 4*E*) whereas the cellular [^{3}H]palmitic acid level decreased ≈10% (Fig. 4*F*), suggesting that the increase of fatty acid in the blood resulted from the direct induction of lipolysis of triglyceride in the adipocytes.

Phenotypes of AIMP1$^{-/-}$ Mice Related to Glucose Metabolism. To address whether the suggested activity of AIMP1 is also observed *in vivo*, we analyzed various metabolites using AIMP1-deficient mice. The construction details of AIMP1$^{-/-}$ mice were described previously (7). The AIMP1-deficient mice displayed diverse phenotypes because of the pleiotropic activity of AIMP1.

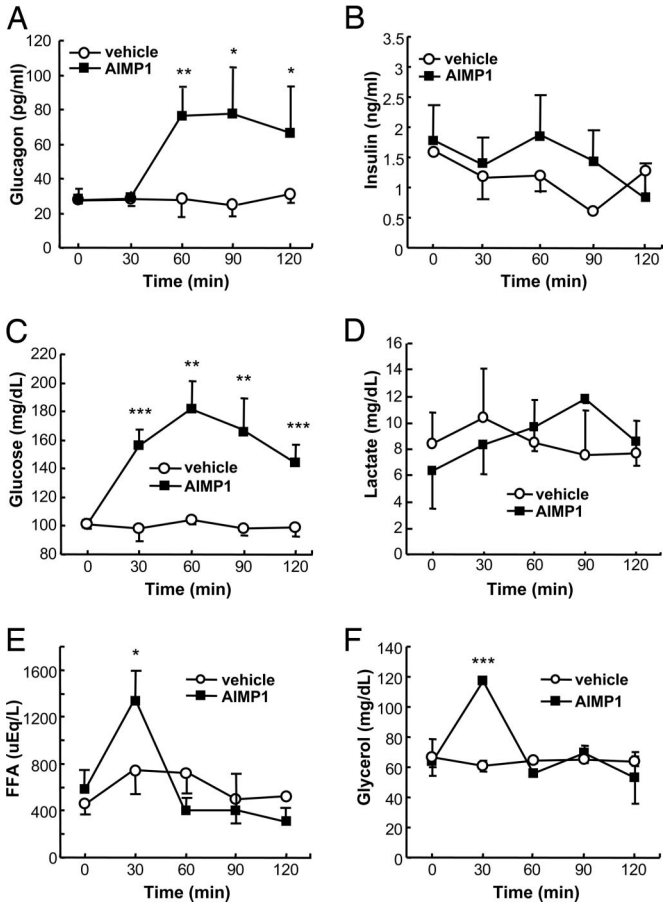

Fig. 3. The effect of AIMP1 on the blood levels of hormones and metabolites related to glucose metabolism. Sprague–Dawley rats were cannulated with AIMP1 for 2 h as described in *Materials and Methods*, blood was collected at the indicated time points, and plasma was obtained by centrifugation. We then measured the plasma levels of glucagon (*A*), insulin (*B*), glucose (*C*), lactate (*D*), free fatty acid (*E*), and glycerol (*F*) using their specific quantification kits ($n = 4$–5). The values are means ± SD. *, $P < 0.07$; **, $P < 0.05$; ***, $P < 0.02$.

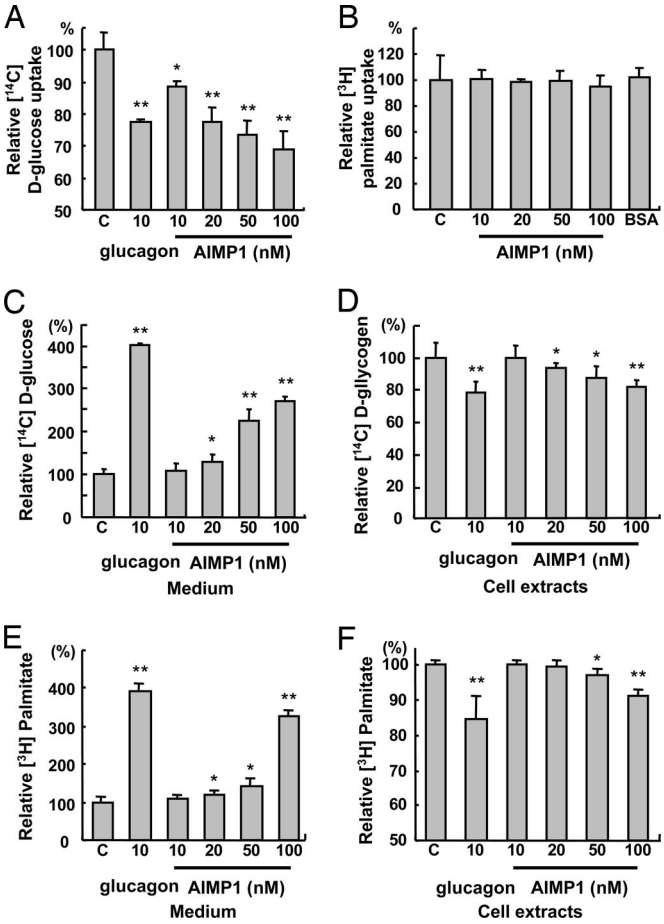

Fig. 4. The effect of AIMP1 on glucose uptake, glycogenolysis, and lipolysis. We treated HepG2 with the indicated concentrations of AIMP1 and assayed the uptake rate of [U-^{14}C]D-glucose (*A*) and [^{3}H]palmitate (*B*). Glucagon was used as a positive control. We stimulated glycogen synthesis in HepG2 with 10 nM insulin, 25 mM D-glucose, and 2 μCi/ml [U-^{14}C]D-glucose for 16 h, and we induced glycogenolysis by incubating cells with glucose-free DMEM containing glucagon or AIMP1 for 4 h. The culture medium (*C*) and cells (*D*) were harvested to quantify [U-^{14}C]D-glucose. We cultured and differentiated 3T3-L1 into adipocytes as described in *Materials and Methods*. We induced the uptake of [^{3}H]palmitate (1 μCi/ml) for 2 h and treated the cells with glucagon or AIMP1 for 7 h. The culture medium (*E*) and adipocytes (*F*) were harvested to measure [^{3}H]palmitate as described in *Materials and Methods*. The values are means ± SD. *, $P < 0.06$; **, $P < 0.01$.

Among them, we focused here on the phenotypes that are thought to be closely associated with glucose metabolism. The growth of AIMP1$^{-/-}$ mice after birth is retarded compared with AIMP1$^{+/+}$ mice (Fig. 7 *A* and *B*, which is published as supporting information on the PNAS web site). At this stage we do not know whether the growth retardation of the mutant mice is directly related to the hormonal function of AIMP1 because the body size is affected by many different attributes. Although AIMP1$^{-/-}$ mice showed energy expenditure rates per body weight similar to the wild-type mice (data not shown), they showed reduced food intake (males, AIMP1$^{+/+}$ and AIMP1$^{-/-}$, 30.56 ± 5.44 and 16.96 ± 3.59 g/week per mouse; $n = 6$–7; $P < 0.0002$). However, we do not know whether it is the cause or the outcome of growth retardation. Weights of major organs involved in fuel metabolism were reduced proportionally to body weight in AIMP1$^{-/-}$ mice except for perigonadal fat (Fig. 7*C*), and AIMP1$^{-/-}$ mice did not display apparent histological or morphological abnormalities in these organs (Fig. 7 *D–F*). The similar phenotype of reduced body fat was also observed in glucagon receptor-null mice (GCGR$^{-/-}$) (13).

The plasma levels of glucose, free fatty acid, glucagon, and insulin were all reduced in AIMP1$^{-/-}$ compared with those in AIMP$^{+/+}$ mice, although the decreased levels were different (Fig. 8 *A–D*, which is published as supporting information on the PNAS web site). Also, AIMP1$^{-/-}$ mice had an ≈20% higher glycogen content in the liver compared with the AIMP1$^{+/+}$ mice, suggesting that they do not mobilize glycogen efficiently (Fig. 8*E*). The metabolite differences shown in AIMP1$^{-/-}$ mice are consistent with the suggested activity of AIMP1 in this work, although the changes are not dramatic under normal feeding conditions. Immunohistochemical staining of pancreatic islets showed that insulin and glucagon are present at normal levels in AIMP1$^{-/-}$ mice, suggesting that AIMP1 would not regulate expression levels of glucagon and insulin (Fig. 9, which is published as supporting information on the PNAS web site). However, upon fasting, the blood glucose concentration was rapidly decreased below 70 mg/dl in AIMP1$^{-/-}$ mice, whereas AIMP1$^{+/+}$ mice maintained a glucose level above 90 mg/dl (Fig. 5*A*). A rapid decrease in glucose in AIMP1$^{-/-}$ mice under starving conditions may result from the defects in glucose compensation, which should be mediated by AIMP1. To check this possibility, we performed an i.p. glucose tolerance test (IPGTT) to compare the glucose sensitivity between AIMP1$^{+/+}$

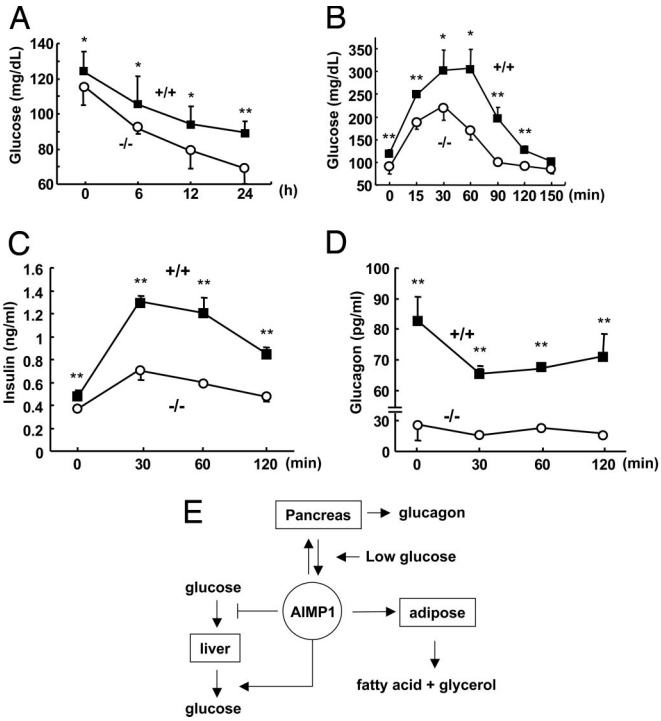

Fig. 5. Genetic depletion of AIMP1 induces hypoglycemia. (*A*) AIMP1$^{+/+}$ and AIMP1$^{-/-}$ mice were fasted for the indicated times, and blood glucose levels were measured ($n = 9$). (*B*) IPGTT in AIMP1$^{+/+}$ and AIMP1$^{-/-}$ mice. Each group of mice was fasted for 14 h, and 2 g of glucose per kilogram of body weight was i.p. injected in a 20% sterile glucose solution. Blood was harvested at the indicated times, and glucose levels were analyzed ($n = 9$). Changes of plasma insulin (*C*) and glucagon (*D*) levels during IPGTT are shown. (*E*) Schematic representation of the hormonal activity of AIMP1 working on different organs for glucose homeostasis. AIMP1 released from the pancreatic α cells at low concentrations of glucose to induce glucagon secretion. AIMP1 inhibits glucose uptake, induces glycogenolysis in the liver, and stimulates lipolysis in adipocytes to increase blood levels of glucose. The values are means ± SD. *, $P < 0.06$; **, $P < 0.05$.

and AIMP1$^{-/-}$ mice. AIMP1$^{-/-}$ mice showed faster removal of glucose from the blood than AIMP1$^{+/+}$ mice (Fig. 5*B*). Responses of insulin and glucagon to IPGTT were much lower in AIMP1$^{-/-}$ mice (Fig. 5 *C* and *D*). In summary, AIMP1 appears to work for the homeostasis of glucose through different organs by inducing glucagon secretion in the pancreas, inhibiting glucose uptake and triggering glycogenolysis in the liver, and stimulating lipolysis in adipose tissue (Fig. 5*E*).

Discussion

Although AIMP1 is a component of the multi-tRNA synthetase complex, AIMP1 levels display significant tissue-dependent variation (Fig. 1*A*), suggesting that AIMP1 may have some unique activities depending on different tissues or organs. In this work we focused on understanding the physiological significance of the pancreatic secretion of AIMP1 and determining its glucagon-like hormonal activity. Genetic depletion of AIMP1 resulted in the dramatic reduction of plasma glucagon levels (Fig. 8*C*), as expected from cellular and *in vivo* experiment results (Figs. 2 and 3), further supporting the idea that AIMP1 is the critical molecule to induce pancreatic secretion of glucagon for blood glucose homeostasis. Although AIMP1 secretion was induced by lowering glucose concentrations in mice (Fig. 2*A*), it did not sensitively respond to the change of glucose concentrations within the range of 90–140 mg/dl in humans (Fig. 10, which is published as supporting information on the PNAS web site), implying that it may work at larger variation of blood glucose in the case of humans. The enhancement of glucose and glucagon usually accompanies the increase of insulin for glucose homeostasis. However, AIMP1 administration did not increase plasma insulin levels (Fig. 3*B*) even when glucagon and glucose levels were enhanced (Fig. 3 *A* and *C*). To determine whether AIMP1 inhibits insulin secretion, we investigated the direct effect of AIMP1 on insulin secretion from pancreatic islets. We found that AIMP1 did not inhibit insulin secretion (Fig. 11, which is published as supporting information on the PNAS web site). Thus, no increase of insulin after AIMP1 infusion might have resulted from its indirect effect. Because AIMP1 is a signaling molecule with complex activity, it may activate various signals that could suppress insulin secretion (14–16).

Glucagon functions through its receptor, which is a member of GTP-binding protein-coupled receptors, and its intracellular signaling is mediated by cAMP, PKA, phosphatidylinositol 3-kinase, and Ca^{2+} even if its downstream signaling pathways are highly complex. Glucagon secretion is also induced by metabolic and hormonal signals involving these molecules (17–19). Although AIMP1 receptor has not been identified yet, AIMP1 activates phosphatidylinositol 3-kinase and PLC and increases intracellular Ca^{2+} levels (20, 21). Based on these observations, AIMP1 appears to induce the secretion of glucagon through the signal pathways that are involved in the exocytosis of glucagon. The phenotypes of the glucose-related metabolism shown in AIMP1$^{-/-}$ mice are similar to those of GCGR$^{-/-}$ mice (13, 22). For instance, GCGR$^{-/-}$ mice showed lower blood glucose levels under fasting conditions than the wild-type mice with little difference under feeding conditions. In addition, exogenously supplemented glucose was more rapidly removed from blood in GCGR$^{-/-}$ mice compared with wild-type mice (13). The phenotypic similarity between the two mutant mice further supports the glucagon-like activity of AIMP1. AIMP1 thus can be used to rescue acute hypoglycemia, which is a critical concern for patients with diabetes.

Although AIMP1 shows functional similarity to glucagon, the two proteins differ in their synthesis, structure, and process. Glucagon is synthesized as preproglucagon in the brain, pancreas, and intestine and is processed through a series of proteolytic cleavage (23–26). In contrast, AIMP1 is ubiquitously present in all type of cells, although it is enriched in a particular set of organs, including the pancreas (Fig. 1), and does not need a proteolytic process for its activation. The multiple activity of AIMP1 as hormone and cytokine is reminiscent of adipokines. For instance, visfatin, previously known as a pre-B cell colony-enhancing factor, is a 52-kDa cytokine that is expressed in lymphocytes (27). As a cytokine it works as a B cell growth factor (27). Acute administration of visfatin lowered the blood glucose concentration by reducing the glucose release from hepatocytes as well as increasing the glucose uptake in myocytes and adipocytes (28). Thus, visfatin is considered an insulin-like hormone that controls blood glucose. The administration of the inflammatory cytokine IL-6 also increases blood glucose through the induction of insulin resistance in adipocytes and glucagon in the pancreas (29, 30). Although AIMP1 is similar to those factors in its activity as a cytokine and hormone, its enrichment in pancreatic α cells and glucagon-like activity distinguish it from other known adipokines. Thus, AIMP1 appears to be a critical factor for efficiency and homeostasis not only in protein synthesis but also in energy metabolism of mammalian systems.

Materials and Methods

Western Blotting of Mouse Tissues. Various isolated mouse organs were placed in RIPA buffer containing 20 mM Tris·HCl (pH 7.6), 150 mM NaCl, 10% glycerol, 1% Triton X-100, 0.1% SDS, 0.5% sodium deoxycholate, 1 mM EDTA, 1 mM PMSF, 5 μg/ml

aprotinin, 5 μg/ml chymostatin, 5 μg/ml leupeptin, 1 mM NaF, 1 mM sodium orthovanadate, and 12 mM β-glycerophosphate, minced with sharp-point scissors, and lysed with a Dounce homogenizer. The lysates were centrifuged at 26,000 $\times$ *g* for 20 min at 4°C. The protein concentrations in the supernatants were quantified by Bradford assay and subjected to Western blotting with antibodies specific to human AIMP1, glutaminyl-tRNA synthetase, and methionyl-tRNA synthetase.

Gel Filtration. Mice tissues were isolated, washed with cold PBS twice, and suspended in lysis solution containing 10 mM Hepes (pH 7.6), 10 mM KCl, 1.5 mM $MgCl_2$, 0.5 mM EGTA, 10 mM NaF, 1 mM PMSF, and protease inhibitor mixture (Roche, Mannheim, Germany). The tissues were then lysed by using a Dounce homogenizer, and the lysates were centrifuged at 23,000 $\times$ *g* for 15 min. The supernatants were mixed with an equal volume of 10 mM Hepes buffer (pH 7.6) containing 150 mM KCl, 1.5 mM $MgCl_2$, 0.5 mM EGTA, 10 mM NaF, 1 mM PMSF, and protease inhibitor mixture (Roche). The samples were filtered through a 0.22-μm membrane, and the proteins were concentrated to 9 mg/ml by using a Vivaspin protein concentrator (Sartorius, Epsom, U.K.). Then the proteins were subjected to gel-filtration chromatography using Sephacryl S-300 (high resolution with the separation range of 10–1,500 kDa) in FPLC (Amersham Pharmacia, Uppsala, Sweden). The eluted fractions were subjected to Western blotting with antibodies specific to each of the components of the multi-tRNA synthetase complex.

Electron Microscopy with ImmunoGold Staining. Pancreases were dissected from mice in 10 mM PBS (pH 7.4) and fixed in a 2% paraformaldehyde/2.5% glutaraldehyde mixture in 10 mM PBS at 4°C for 2 h. After being washed with PBS three times at 30-min intervals the tissues were dehydrated in ethanol. The dehydrated tissues were then embedded in LR White (London Resin, Theale, U.K.) in gelatin capsules. For electron microscopic examination, the embedded tissues were thin-sectioned with an ultramicrotome (LKB, Mt. Waverley, Victoria, Australia) and attached to nickel grids. After incubation with PBSTB (10 mM PBS containing 0.05% Tween 20 and 1% BSA) for 10 min, the grids were reacted with rabbit anti-AIMP1 or mouse anti-glucagon antibody diluted 50-fold with PBSTB and then washed six times with PBSTB to remove nonspecifically bound antibodies. The grids were reacted with 20 nm of protein A-conjugated colloidal gold (Sigma, St. Louis, MO) probes diluted 25-fold with PBSTB (31, 32). After being washed with PBST containing 10 mM PBS, 0.05% Tween 20, and distilled water three times, the labeled sections were contrasted with 2% uranyl acetate and observed under an electron microscope (JEOL, Seoul, Korea) at 80 kV.

Immunohistochemical Staining. Pancreases were isolated from mice and fixed in 10% formaldehyde for 24 h. The fixed tissues were dehydrated and embedded in paraffin. We then sliced the embedded tissues with a microtome (Leica, Deerfield, IL), mounted them on silane-coated slides, and dewaxed and rehydrated them. The slides were equilibrated with PBS, blocked with PBS containing 0.1% Tween 20 and 1% skim milk for 1 h at room temperature, and reacted with specific antibodies against AIMP1, glucagon (Sigma), and insulin (Sigma) at room temperature for 2 h. We washed the slides with PBS containing 0.1% Tween 20 and incubated them at 37°C for 1 h with FITC- or rhodamine- or biotin-conjugated secondary antibody. The nuclei were counterstained with propidium iodide (10 μg/ml) for 10 min, and the slides were examined under a confocal immunofluorescence microscope (μ-Radiance, Bio-Rad, Hercules, CA). Biotin-conjugated secondary antibodies were captured with streptavidin-HRP and developed with QEC solution (Zymed, South San Francisco, CA). The nuclei were counterstained with Meyer's hematoxylin.

IPGTT. AIMP1$^{+/+}$ and AIMP1$^{-/-}$ mice between 12 and 16 weeks old were fasted for 14 h starting at the beginning of the light cycle. The mice were not anesthetized. At time 0 blood glucose was measured, and immediately thereafter a 20% sterile glucose solution was injected i.p. to reach a concentration of 2 g/kg of body weight. Blood was collected at the indicated time points, and glucose levels were measured.

Cardiac Perfusion. Twelve-week-old male mice (C57BL/6) were anesthetized with an i.p. injection of 2.5% avertin (100 μl per 10 g). The abdomen was incised with sterile scissors to inject the left ventricle with 26-gauge needles filled with conditioned medium. We cut the vena cava and perfused the heart with the indicated glucose solutions at a flow rate of 10 ml/min for 10 min. We isolated the pancreases, washed them with PBS containing 1% streptomycin/penicillin, and incubated them on the conditioned medium for 2 h in a CO_2 incubator at 37°C. We harvested the medium, precipitated proteins by the addition of 10% TCA at room temperature for 2 h, and centrifuged at 16,000 $\times$ *g* for 15 min. We separated the protein extracts by 10% SDS/PAGE and blotted them with anti-AIMP1 antibody.

AIMP1 Secretion from Pancreatic α Cells. We purchased aTC1 clone 9 from American Type Culture Collection (Manassas, VA) and maintained the cells in modified DMEM according to the recommendation of American Type Culture Collection. The cells were plated on 60-mm dishes and cultured for 4 days. We exchanged the medium with serum-free DMEM containing high glucose (450 mg/dl) or low glucose (75 mg/dl), harvested the medium at specified time intervals, and centrifuged the medium at 3,000 $\times$ *g* for 15 min and 16,000 $\times$ *g* for another 15 min to remove contaminants. We precipitated proteins from the supernatants with 10% TCA for 2 h at room temperature and centrifuged them at 16,000 $\times$ *g* for 15 min. Then we harvested the pellets and resuspended them with 10 mM Tris·HCl (pH 8.3). We loaded the suspension for 10% SDS/PAGE and transferred it to a PVDF membrane for immunoblotting with anti-AIMP1 antibody.

Adipocyte Differentiation. Preadipocyte 3T3-L1 was cultured in DMEM containing 10% FBS and 1% penicillin/streptomycin in a humidified 5% CO_2 incubator. The cells were seeded onto 12 multiwell plates, cultured to confluency, and maintained for 2 days. The medium was exchanged with the differentiation medium [DMEM containing 0.5 mM 3-isobutyl-1-methylxanthine (Sigma), 1 μM dexamethasone (Sigma), and 10 μg/ml bovine insulin (Sigma)] for 2 days and replaced every other days for 6 days. For lipolysis assay, the cells were washed with PBS and cultured with serum-free DMEM containing 1 μCi/ml [^{3}H]BSA-palmitate (1 Ci = 37 GBq) and 10 nM bovine insulin for 2 h. The cells were washed with PBS and cultured with serum-free DMEM containing glucagon or AIMP1 for 8 h. The medium was harvested to measure the released palmitate, and the cells were washed with PBS and lysed with 0.5 N NaOH. [^{3}H]Palmitate was quantified by using a liquid scintillation counter (LKB), and the cellular concentration of [^{3}H]palmitate was calibrated with the protein concentration.

Glycogenolysis Assay. We maintained HepG2 in the MEM containing 10% FBS and 1% penicillin/streptomycin in a humidified 5% CO_2 incubator. We seeded HepG2 (2×10^6) cells onto a six-well plate and cultured them for a glycogenolysis assay. The medium was replaced with serum-free MEM containing 25 mM glucose, 10 nM insulin, and [U-^{14}C]D-glucose (2 μCi/ml) and cultured for 16–18 h. The cells were washed with HBS and

incubated with glucose-free DMEM containing glucagon or AIMP1 for 4 h. For the glucose release assay the medium was harvested and precipitated with 10% TCA, and the supernatant was taken for the counting of the released [U-^{14}C]glucose. For cellular glucose assay, the cells were washed with HBS and lysed with 1 N NaOH. Radioactivity was quantified by using a liquid scintillation counter (LKB), and the cellular concentration of [U-^{14}C]glucose was calibrated with the protein concentration.

AIMP1 Infusion. Male Sprague–Dawley rats (250–300 g) were purchased and maintained on a 12-h dark/12-h light cycle at 22°C. We fasted the rats for 5 h to perform the infusion experiment through the cannulation of tail veins. First we infused 3.6 mg/kg by bolus injection with AIMP1 for 1 min and harvested blood at indicated time points for metabolic analysis. We centrifuged the blood at 2,000 × *g* for 20 min, harvested the plasma, and stored it at −70°C.

Glucagon Secretion Assay. aTC1 clone 9 cells were cultured with modified DMEM containing 4 mM L-glutamine, 3.0 g/liter glucose, 1.5 g/liter sodium bicarbonate, 15 mM Hepes, 0.1 mM nonessential amino acids, 0.02% BSA, 10% heat-inactivated dialyzed FBS, and 1% penicillin/streptomycin in a humidified 5% CO_2 incubator. We seeded aTC1 clone 9 cells on six-well plates, cultured them for 4 days, and changed them with serum-free medium. We treated the cells with 100 nM AIMP1 and harvested the medium at the indicated times. We quantified the secreted glucagon by using a glucagon RIA kit (LINCO Research, St. Charles, MO) following the manufacturer's instructions.

Fatty Acid Uptake Assay. We cultured C2C12 cells in DMEM containing 10% FBS and 1% penicillin/streptomycin, and we changed the medium with DMEM containing 2% horse serum. We cultured the cells and changed the medium every other day for 5 days. Adipocyte differentiation of 3T3-L1 and HepG2 cells was described above. Myotubes were stimulated with the indicated concentrations of AIMP1 in serum-free medium for 30 min, and we treated [^{3}H]BSA-palmitate (1 μCi per well) for 4 min. For adipocytes, we changed the culture medium with serum-free medium and incubated the cells for 2 h. We treated AIMP1 for 30 min and induced the incorporation of [^{3}H]BSA-palmitate (1 μCi per well) for 4 min. We washed the cells with HBS and lysed them with 1 N NaOH. Radioactivity was quantified by using a liquid scintillation counter (LKB).

Glucose Uptake. We cultured HepG2, myotubes, and adipocytes as described above. Glucose uptake was performed as described (33). Briefly, the cells were starved in serum-free medium for 2 h and treated with AIMP1 for 30 min. We added [U-^{14}C]D-glucose (1 μCi per well) and quantified the incorporation rate.

Lipolysis Assay. We induced the differentiation of 3T3-L1 cells to adipocytes for 4 days, changed the medium, and cultured the cells with DMEM containing 10% FBS, 1% penicillin/streptomycin, 5 μg/ml insulin, and [^{3}H]palmitate (1 μCi per well) for 3 h. We washed the cells with serum-free medium three times and stimulated them with AIMP1 or glucagon for 8 h. We harvested the medium and cell lysates, and [^{3}H]palmitate in each fraction was quantified by using a liquid scintillation counter (LKB).

Statistical Analyses. Data are means ± SD. Statistical significance was assessed by Student's *t* test.

This work was supported by a grant from the National Creative Research Initiatives of the Ministry of Science and Technology, Korea.

1. Deutscher MP (1974) *Methods Enzymol* 29:577–583.
2. Dang CV, Yang DC (1982) *Int J Biochem* 14:539–543.
3. Mirande M, Gache Y, Le Corre D, Waller JP (1982) *EMBO J* 1:733–736.
4. Yang DC, Garcia JV, Johnson YD, Wahab S (1985) *Curr Top Cell Regul* 26:325–335.
5. Park SG, Jung KH, Lee JS, Jo YJ, Motegi H, Kim S, Shiba K (1999) *J Biol Chem* 274:16673–16676.
6. Ko Y-G, Park H, Kim T, Lee J-W, Park SG, Seol W, Kim JE, Lee W-H, Kim S-H, Park JE, Kim S (2001) *J Biol Chem* 276:23028–23033.
7. Park SG, Shin H, Shin YK, Lee Y, Choi EC, Park BJ, Kim S (2005) *Am J Pathol* 166:387–398.
8. Barnett G, Jakobsen AM, Tas M, Rice K, Carmichael J, Murray JC (2000) *Cancer Res* 60:2850–2857.
9. Park SG, Kang YS, Ahn YH, Lee SH, Kim KR, Kim KW, Koh GY, Ko YG, Kim S (2002) *J Biol Chem* 277:45243–45248.
10. Park H, Park SG, Lee J-W, Kim T, Kim G, Ko Y-G, Kim S (2002) *J Leukocyte Biol* 71:223–230.
11. Favorova OO, Zargarova TA, Rukosuyev VS, Beresten SF, Kisselev LL (1989) *Eur J Biochem* 184:583–588.
12. Beresten SF, Filonenko VV, Favorova OO (1991) *Biokhimiya (Moscow)* 56:1155–1189.
13. Gelling RW, Du XQ, Dichmann DS, Romer J, Huang H, Cui L, Obici S, Tang B, Holst JJ, Fledelius C, *et al.* (2003) *Proc Natl Acad Sci USA* 100:1438–1443.
14. Cheng H, Straub SG, Sharp GW (2003) *Am J Physiol* 285:E287–E294.
15. Sharp GW (1996) *Am J Physiol* 271:C1781–C1799.
16. Vara E, Tamarit-Rodriguez J (1989) *Am J Physiol* 257:E923–E929.
17. Aromataris EC, Roberts ML, Barritt GJ, Rychkov GY (2006) *J Physiol* 573:611–625.
18. Jiang G, Zhang BB (2003) *Am J Physiol* 284:E671–E678.
19. Ma X, Zhang Y, Gromada J, Sewing S, Berggren PO, Buschard K, Salehi A, Vikman J, Rorsman P, Eliasson L (2005) *Mol Endocrinol* 19:198–212.
20. Kao J, Fan Y-G, Haehnel I, Brett J, Greenberg S, Clauss M, Kayton M, Houck K, Kisiel W, Seljelid R, *et al.* (1994) *J Biol Chem* 269:9774–9782.
21. Park H, Park SG, Kim J, Ko YG, Kim S (2002) *Cytokine* 20:148–153.
22. Parker JC, Andrews KM, Allen MR, Stock JL, McNeish JD (2002) *Biochem Biophys Res Commun* 290:839–843.
23. Furuta M, Zhou A, Webb G, Carroll R, Ravazzola M, Orci L, Steiner DF (2001) *J Biol Chem* 276:27197–27202.
24. Rouille Y, Bianchi M, Irminger JC, Halban PA (1997) *FEBS Lett* 413:119–123.
25. Rouille Y, Kantengwa S, Irminger JC, Halban PA (1997) *J Biol Chem* 272:32810–32816.
26. Rouille Y, Westermark G, Martin SK, Steiner DF (1994) *Proc Natl Acad Sci USA* 91:3242–3246.
27. Samal B, Sun Y, Stearns G, Xie C, Suggs S, McNiece I (1994) *Mol Cell Biol* 14:1431–1437.
28. Fukuhara A, Matsuda M, Nishizawa M, Segawa K, Tanaka M, Kishimoto K, Matsuki Y, Murakami M, Ichisaka T, Murakami H, *et al.* (2005) *Science* 307:426–430.
29. Rotter V, Nagaev I, Smith U (2003) *J Biol Chem* 278:45777–45784.
30. Tsigos C, Papanicolaou DA, Kyrou I, Defensor R, Mitsiadis CS, Chrousos GP (1997) *J Clin Endocrinol Metab* 82:4167–4170.
31. Gosselin EJ, Sorenson GD, Dennett JC, Cate CC (1984) *J Histochem Cytochem* 32:799–804.
32. Bendayan M, Duhr MA (1986) *J Histochem Cytochem* 34:569–575.
33. Kase ET, Wensaas AJ, Aas V, Hojlund K, Levin K, Thoresen GH, Beck-Nielsen H, Rustan AC, Gaster M (2005) *Diabetes* 54:1108–1115.